J. Opt. A: Pure Appl. Opt. **11** (2009) 075101 (6pp) doi:10.1088/1464-4258/11/7/075101

Subwavelength internal imaging by means of a wire medium

Yan Zhao, Pavel Belov and Yang Hao

School of Electronic Engineering and Computer Science, Queen Mary, University of London, Mile End Road, London E1 4NS, UK

E-mail: yan.zhao@elec.qmul.ac.uk

Received 20 November 2008, accepted for publication 13 February 2009
Published 15 April 2009
Online at stacks.iop.org/JOptA/11/075101

Abstract
In this paper, the phenomenon of evanescent wave amplification inside a half-wavelength-thick wire medium slab is studied numerically and used for subwavelength imaging of objects at significant distances from the lens. The wire medium is analysed using both a spatially dispersive finite-difference time-domain (FDTD) method employing the effective medium theory and a full-wave commercial electromagnetic simulator CST Microwave Studio™ modelling the physical structure. It is demonstrated that subwavelength details of a source placed at a distance $\lambda/10$ from a wire medium slab can be detected inside the slab with a resolution of approximately $\lambda/10$ in spite of the fact that they cannot be resolved at the front interface of the device, due to the rapid decay of evanescent spatial harmonics in free space. The influence of different distances between the source and the wire medium on the internal imaging property is also addressed.

Keywords: finite-difference time-domain, metamaterial, subwavelength internal imaging, wire medium

(Some figures in this article are in colour only in the electronic version)

1. Introduction

Conventional imaging systems are restricted by the so-called diffraction limit: any source details below the half-wavelength at the frequency of operation cannot be resolved at the image plane. However, it has been proposed in [1] that a planar lens formed by left-handed material (LHM) [2] can be used to image source information with a spatial resolution below the diffraction limit. A lens formed by LHM with $\varepsilon = \mu = -1$ is termed a 'perfect lens', and the principle of its operation is based on the negative refraction of propagating waves and the amplification of evanescent field components [1]. It is well known that evanescent waves carry subwavelength source details and decay exponentially in positive-index materials. The uniqueness of an LHM is that the evanescent waves show a growing behaviour when propagating within the medium. Hence the subwavelength details which are lost in the region between the source and a perfect lens can be restored to create a perfect image [1]. The amplification of evanescent waves in an LHM is due to the resonant excitation of surface plasmons at the interfaces. However, such an effect is sensitive to the losses in the LHM, and thus limits the maximum thickness of the LHM slab [3]. Furthermore, the mismatch of the LHM with its surrounding medium also limits the imaging capability of LHM lenses [4].

Recently, it has been suggested to use an alternative way to transport subwavelength source details to an image plane at a significant distance. The principle of operation, referred to as 'canalization' [5], is based on the fact that, for a certain type of device, the evanescent wave components can be transformed into propagating waves, and therefore the source field can be delivered to its back interface with little or no deterioration. In contrast to the case of an LHM, such devices are less sensitive to losses. Recent works on the subwavelength imaging using anisotropic materials (operating in the canalization regime) include [6–8]. Moreover, the work presented in [9] shows that introducing nonlinearity suppresses the diffraction, and is useful for future subwavelength imaging devices even when the dispersion curve is not flat.

One typical example of the structures operating in the canalization regime is the wire medium formed by an array of parallel conducting wires [10]. The thickness of the wire

medium needs to be equal to an integer multiple of half-wavelengths at the operating frequency (due to the Fabry–Perot resonance) in order to avoid reflections between the source and the structure. It has been demonstrated experimentally and numerically that such a canalization regime does indeed exist, and subwavelength details can be transported through the wire medium at frequencies up to the terahertz (THz) and infrared range [11–13].

In addition to the canalization regime, another interesting phenomenon of the wire medium is observed from numerical simulations and presented in this paper: the evanescent waves can be amplified *inside* the wire medium. Hence the effect of images appearing inside the wire medium slab is called 'internal imaging'. The previously investigated subwavelength imaging property of the wire medium, i.e. images appearing at the back interface, is highly dependent on the distance between the source and the wire medium, and the external images disappear when the distance increases. Due to the internal imaging effect, the subwavelength imaging capability of the wire medium can be further improved. In contrast to the case of LHM lenses where the amplification of evanescent waves is due to the resonant excitation of surface plasmons, the amplification of evanescent waves in a wire medium slab is a result of the resonant excitation of standing waves inside the slab. Although the internal imaging effect also exists in LHM slabs (there are two focal points, at both the inside and the outside of LHM lenses), as mentioned above, the practical realization of LHM lenses has many difficulties. On the other hand, the internal imaging capability of the wire medium can be used for subwavelength imaging of objects at significant distances from the lens. In the following, we first present the numerical simulation results using a spatially dispersive finite-difference time-domain (FDTD) method developed in [14], where the effective medium theory is used and microstructures of the wire medium are neglected. Hence the FDTD method has better efficiency compared with simulations modelling microstructures. Then the FDTD simulation results are validated by a commercial simulation package CST Microwave Studio™ modelling the actual physical structure of the wire medium[1].

2. Spatially dispersive FDTD simulations of internal imaging by the wire medium

The simulation of the wire medium can be performed either by modelling the physical structure, i.e. parallel conducting wires, or using the effective medium theory, so that the wire medium can be represented by a homogeneous dielectric slab provided that the inner spacing of wires is much smaller than the wavelength of interest. In this section, we demonstrate the internal imaging phenomenon numerically using the effective medium theory by applying the spatially dispersive FDTD method [14]. Modelling the physical structure based on a commercial simulation package CST Microwave Studio™ is introduced in section 3.

The wire medium can be approximated as a homogeneous dielectric slab with both frequency and spatial dispersions. In this paper we use the following expression for the permittivity tensor derived in [16]:

$$\varepsilon(\omega, \mathbf{q}) = \mathbf{xx} + \varepsilon(\omega, q_y)\mathbf{yy} + \mathbf{zz},$$
$$\varepsilon(\omega, q_y) = 1 - \frac{k_\mathrm{p}^2}{k^2 - q_y^2}, \tag{1}$$

where the y-axis is oriented along the wires, q_y is the y-component of the wavevector $\mathbf{q}$, $k = \omega/c$ is the wavenumber of free space, c is the speed of light, and k_p is the wavenumber corresponding to the plasma frequency of the wire medium. The wavenumber k_p depends on the lattice periods a and b, and on the radius of the wires, r [17]:

$$k_\mathrm{p}^2 = \frac{2\pi/(ab)}{\ln\frac{\sqrt{ab}}{2\pi r} + F(a/b)},$$
$$F(\xi) = -\frac{1}{2}\ln\xi + \sum_{n=1}^{+\infty}\left(\frac{\coth(\pi n\xi) - 1}{n}\right) + \frac{\pi}{6}\xi. \tag{2}$$

For the case of a square grid ($a = b$), $F(1) = 0.5275$ and the expression (2) reduces to

$$k_\mathrm{p}^2 = \frac{2\pi/a^2}{\ln\frac{a}{2\pi r} + 0.5275}. \tag{3}$$

The expression (1) for the permittivity tensor of the wire medium is valid and the structure is non-magnetic if the wires are thin as compared to the lattice periods (when the polarization across the wires is negligibly small as compared to the longitudinal polarization) and if the lattice periods are much smaller than the wavelength (when the wire medium can be homogenized).

A spatially dispersive FDTD method has been developed [14] to take into account the spatial dispersion effect in the wire medium [16]. We have applied the spatially dispersive FDTD method to analyse the subwavelength imaging property of the wire medium [14]. In this paper, we extend the method to three dimensions to study the internal imaging property of the wire medium.

The computation domain in the FDTD simulations is shown in figure 1 (except that the wire medium is modelled as a bulk material instead of as parallel thin wires). The wavenumber corresponding to the plasma frequency is chosen as $k_\mathrm{p} = 6k$, where $k = 2\pi\lambda$ and λ is the operating wavelength of the wire medium slab in simulations. A crown-shaped near-field source is applied in the simulations and it is placed at a distance d to the front interface of the wire medium. The distance d varies from $\lambda/15$, $\lambda/10$, to $\lambda/7$. The source is modelled as segments of perfect electric conductor (PEC) using staircase approximations, and it is excited at the bottom left corner using a delta-gap excitation in the FDTD simulation [18]. The radius of the PEC wires is the same as the FDTD cell size, which is fixed at $\lambda/100$ for all FDTD

[1] During the review process of this paper, the generalized theory of the evanescent wave enhancement inside materials with extreme anisotropy (the wire medium is a typical example of such materials) was studied and presented in detail in [15].

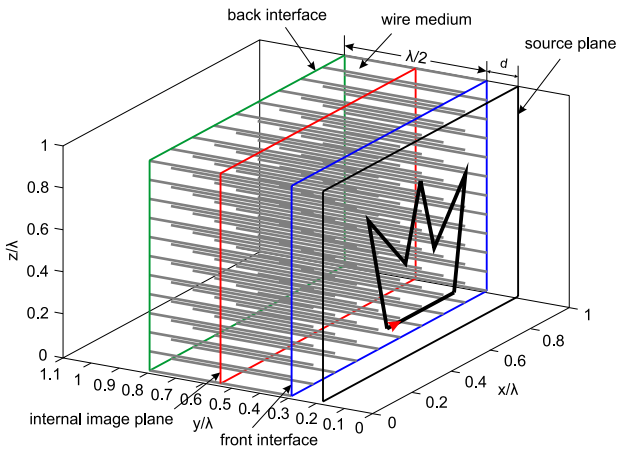

Figure 1. A three-dimensional (3D) FDTD simulation domain for the modelling of internal subwavelength imaging by a wire medium slab with thickness $\lambda/2$ and infinite transverse dimensions.

simulations. The time step is chosen according to the Courant stability criterion [18]. Berenger's perfectly matched layer (PML) [19] is employed to truncate the outer boundary of the simulation domain along y-direction and the modified PML [20] is applied to model infinite wire medium slabs along the x- and z-directions and reduce the convergence time in simulations [20]. The dimensions of the simulation domain in the x- and z-directions are $2\lambda/3 \times 2\lambda/3$. The thickness of the wire medium slab is chosen as $\lambda/2$ to achieve good impedance matching between the source and the structure. As shown in figure 1, the middle plane of the wire medium is defined as the internal image plane. It has been demonstrated that the wire medium can image the electric field component along the wires [10]. Inside the wire medium, the field distribution has TEM polarization (transverse electric and magnetic modes with respect to the orientation of wires) and it is formed by the so-called transmission-line modes [5]. The electric field components of such modes are zero along the wires (but the electric displacement is non-zero). Therefore, in figure 2 we plot the distributions of electric field only at the source plane and the front interface, but at the internal image plane the electric displacement (normalized to the free space permittivity) is plotted instead. It is equivalent to the electric current density flowing along the wire since $D_y = \varepsilon_0 E_y + J_y/(\mathrm{j}\omega)$. The field distributions at various planes are calculated according to different distances d between the source and the wire medium and plotted after the steady state is reached in simulations.

It is clearly seen that the crown-shaped source creates a subwavelength field distribution at the source plane; however, it becomes blurred at the front interface of the wire medium due to the spatial decay of the evanescent spatial harmonics in the free space region, especially for the case of $d = \lambda/7$, when the distribution at the front interface can hardly be identified. The wire medium operates in the canalization regime and the electric field distribution at the back interface is repeated at the front one; however, such a field distribution does not create a sharp image of the original source. The surprising result is that, inside the wire medium, lost subwavelength details can be recovered due to the amplification of evanescent wave components. In contrast to the case of LHM slabs, all incident evanescent spatial harmonics inside the wire medium are transformed into propagating waves, independent of their transverse variations. The thickness of the wire medium slab is tuned to the Fabry–Perot resonance. As a result, the evanescent waves excite standing waves inside the slab, and in this case they are amplified due to the natural resonance of the wire medium slab. It can be identified from figure 2 that the resolution of the internal images is about $\lambda/10$.

Internal images with good subwavelength resolutions are observed when the source is placed close to the wire medium slab (i.e. $d < \lambda/15$). If the distance is increased to $\lambda/10$ and even $\lambda/7$, the internal images do not contain enough subwavelength details of the source. We conclude that internal imaging with good subwavelength resolution is available only for a limited range of distances between the source and the wire medium, because the dependence of the transfer function for the evanescent spatial harmonics on the transverse wavevector is linear rather than exponential as for the case of LHM [1].

In the above analysis, we have assumed the wire medium to be a homogeneous dielectric material. However, in practice, since the electric displacement inside the wire medium is proportional to the currents flowing along the wires, in order to detect the internal images, one needs to measure the current density instead of either the electric or magnetic field, in contrast to the canalization regime, where the image is formed at the back interface of the wire medium and can be detected using near-field scanning. In section 3, we model the physical structure of the wire medium and demonstrate numerically that the currents along the wires indeed carry the subwavelength details of a source.

3. Simulations of internal imaging by modelling the physical structure of the wire medium

In the simulations using CST Microwave Studio™, the overall dimensions of the wire medium and the crown-shaped source are kept the same as in section 2 using the FDTD method. The number of wires is 21×21 along the x- and z-directions, respectively, and the inner spacing between wires is $a = \lambda/30$. The radius of the wires is $r = \lambda/300$. The wavenumber corresponding to the plasma frequency can be estimated from equation (2) as $k_\mathrm{p} \approx 75k$, where k is the wavenumber corresponding to the operating wavelength λ in simulations. We also consider three different distances between the source and the wire medium: $d = \lambda/15$, $\lambda/10$, and $\lambda/7$. The normalized distributions of the y-component of the electric field at the source plane and at the front interface, as well as the current density along the wires (the currents are converted to field intensities to compare with the other two distributions) in the middle plane of the wire medium are shown in figure 3. It is shown that the source distribution is much sharper compared to the FDTD simulation results. This is due to the fine mesh used in the CST simulations in order to model thin wires accurately. Again we observe similar distributions at the front interface of the wire medium where less detail of the source can be detected. The current density is plotted on discrete grids (the

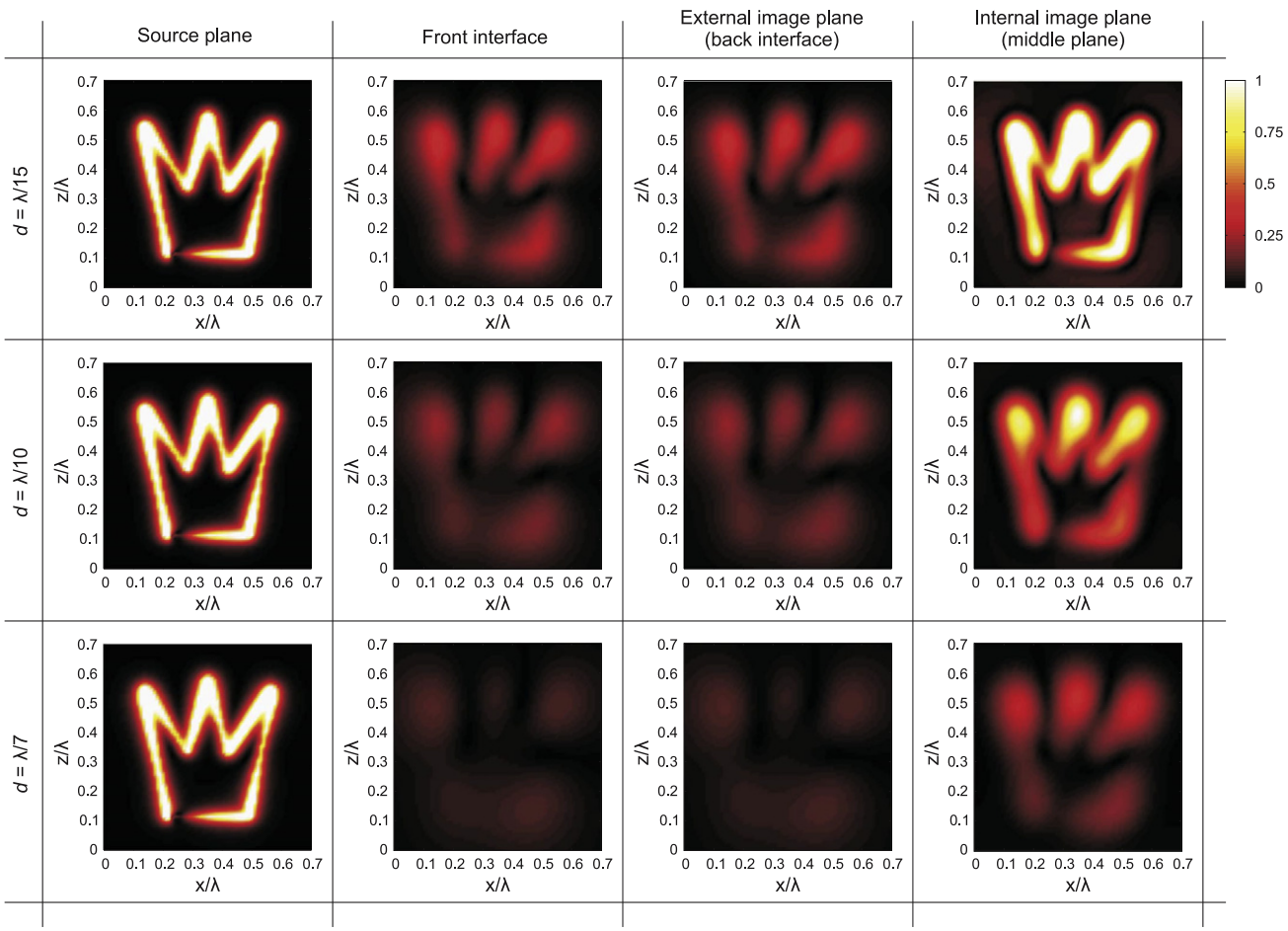

Figure 2. Normalized distributions of the y-component of the electric field at the source plane, the front interface, and the electric displacement at the internal image plane of the wire medium for different distances between the source and the wire medium calculated from spatially dispersive FDTD simulations.

third column in figure 3) since only 21×21 wires are present in the modelled wire medium. The current density shows significant enhancement compared to the field distributions at the front interface of the wire medium, which demonstrates the internal subwavelength imaging capability of the wire medium.

The low image resolution of the internal current density distribution is due to the insufficient number of sampling points (21×21). Therefore, to acquire a higher resolution of internal images, one can use the wire medium formed by more densely packed wires. For example, we have considered a wire medium formed by 41×41 wires with the spacing between the wires $a = \lambda/60$, keeping the transverse dimension of the wire medium the same as the previous case. According to equation (2), the plasma frequency is higher for this case, and therefore one could expect images with a higher resolution. However, the wire density cannot be increased arbitrarily due to the fact that, when the filling ratio of wires increases, the structure may exhibit anisotropic magnetic properties [21–23]. The influence of the material parameter change on the subwavelength imaging property of the wire medium is currently under investigation.

The current density distributions from CST simulations for the case of 41×41 wires are plotted in figure 4. Note that, for illustration purposes, the distributions are not normalized. It can be seen that, by increasing the density of wires, the internal image resolution can be improved, which is especially useful when a more complex source is considered.

The preliminary estimations show that the image appears near the middle plane of the $\lambda/2$ thick wire medium slab and does not change significantly even when the image plane is offset from the middle plane by 5–10%. The plane of the best image formation cannot be determined precisely from numerical simulations since the distribution of electric displacement or current density inside the wire medium varies slowly along the direction of wires. In this paper, we have considered a wire medium slab with a half-wavelength thickness. For wire medium slabs with greater thicknesses (an integer multiple of a half-wavelength), there are multiple planes for the internal imaging, where the evanescent spatial harmonics generated by the source can be amplified and the information lost in the free space region can be restored. The number of internal image planes can be given by N if the thickness of the wire medium is $N\lambda/2$. The distance of the internal image planes to the front interface of the wire medium can be approximately given by $(2n-1)\lambda/4$, where $n = 1, 2, \ldots, N$.

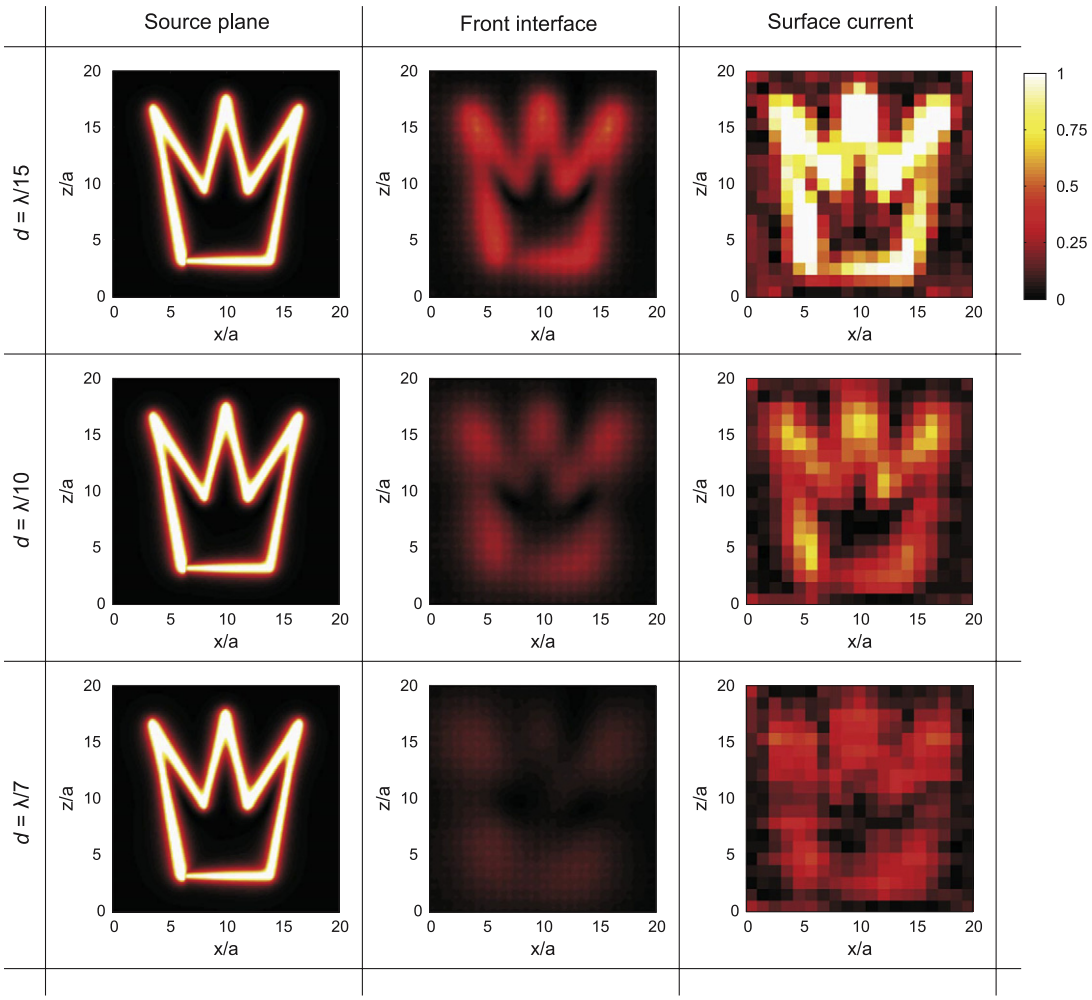

Figure 3. Normalized distributions of the y-component of the electric field at the source plane and the front interface, and the current density at the internal image plane of the wire medium for different distances between the source and the wire medium calculated from CST simulations of the physical structure.

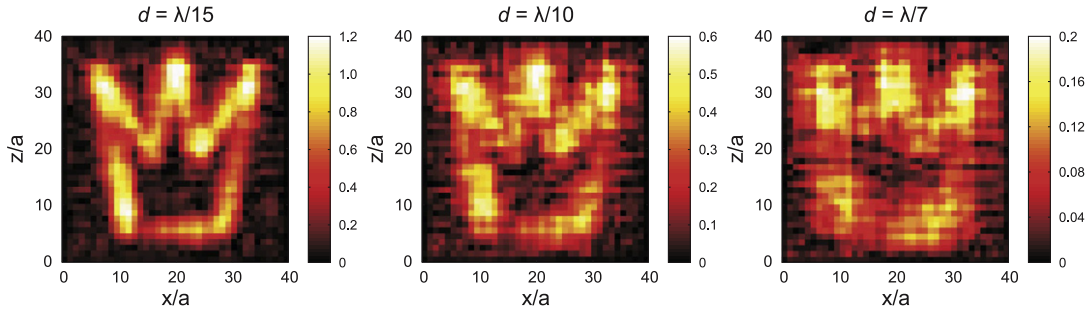

Figure 4. The current density from CST simulations of the physical wire medium (41 × 41 wires) for different distances between the source and the wire medium.

4. Conclusion

The internal imaging capability of the wire medium, i.e. images with a much higher resolution appear inside the wire medium compared with the external ones, is demonstrated numerically by modelling the physical structure and using the effective medium theory: wire medium slabs are capable of imaging a source with subwavelength resolutions located at significant distances from the device. The operational principle of 'internal imaging' is based on the excitation of standing waves inside the wire medium slab rather than the resonance of surface plasmons in LHMs. The results presented in this paper are normalized to wavelength and they are applicable for arrays of metallic rods at frequencies up to THz range since, at these frequencies, most of the metals can be well modelled as perfect electric conductors (PECs) [11, 24]. Similar effects of internal

imaging are expected at infrared frequencies. However, at these frequencies the PEC model is not applicable and the operation of devices may strongly depend on the properties of constituent materials [12, 13]. In practice, it is possible to capture internal images by embedding detectors into metallic wires at the internal image plane and directly measuring the currents flowing along the wires. The internal imaging effect can be used for subsurface imaging and the creation of new generation subwavelength imaging devices. In addition, the wire medium at THz and infrared frequencies can be used as an endoscope for medical applications.

Acknowledgments

The authors would like to thank EPSRC for the financial support and Mr G Palikaras for his help during the preparation of the paper. P A Belov acknowledges the financial support by EPSRC Advanced Research Fellowship EP/E053025/1.

References

[1] Pendry J 2000 Negative refraction index makes a perfect lens *Phys. Rev. Lett.* **85** 3966–9
[2] Veselago V G 1968 The electrodynamics of substances with simultaneously negative values of ε and μ *Sov. Phys.—Usp.* **10** 509–14
[3] Podolskiy V A and Narimanov E E 2005 Near-sighted superlens *Opt. Lett.* **30** 75–7
[4] Smith D R, Schurig D, Rosenbluth M, Schultz S, Ramakrishna S A and Pendry J B 2003 Limitations on subdiffraction imaging with a negative refractive index slab *Appl. Phys. Lett.* **82** 1506
[5] Belov P A, Simovski C R and Ikonen P 2005 Canalization of subwavelength images by electromagnetic crystals *Phys. Rev.* B **71** 193105
[6] Belov P A and Hao Y 2006 Subwavelength imaging at optical frequencies using a transmission device formed by a periodic layered metal-dielectric structure operating in the canalization regime *Phys. Rev.* B **73** 113110
[7] Wood B, Pendry J B and Tsai D P 2006 Directed subwavelength imaging using a layered metal-dielectric system *Phys. Rev.* B **74** 115116
[8] Scalora M *et al* 2007 Negative refraction and sub-wavelength focusing in the visible range using transparent metallodielectric stacks *Opt. Express* **15** 508–23
[9] Liu Y, Bartal G, Genov D A and Zhang X 2007 Subwavelength discrete solitons in nonlinear metamaterials *Phys. Rev. Lett.* **99** 153901
[10] Belov P A, Hao Y and Sudhakaran S 2006 Subwavelength microwave imaging using an array of parallel conducting wires as a lens *Phys. Rev.* B **73** 033108
[11] Shvets G, Trendafilov S, Pendry J B and Sarychev A 2007 Guiding, focusing, and sensing on the subwavelength scale using metallic wire arrays *Phys. Rev. Lett.* **99** 053903
[12] Silveirinha M G, Belov P A and Simovski C R 2007 Subwavelength imaging at infrared frequencies using an array of metallic nanorods *Phys. Rev.* B **75** 035108
[13] Silveirinha M G, Belov P A and Simovski C R 2008 Ultimate limit of resolution of subwavelength imaging devices formed by metallic rods *Opt. Lett.* **33** 1726–8
[14] Zhao Y, Belov P A and Hao Y 2006 Spatially dispersive finite-difference time-domain analysis of sub-wavelength imaging by the wire medium slabs *Opt. Express* **14** 5154–67
[15] Belov P A, Zhao Y, Hao Y and Parini C 2009 Enhancement of evanescent spatial harmonics inside of materials with extreme optical anisotropy and its application for subwavelength imaging *Opt. Lett.* **34** 527–9
[16] Belov P A, Marques R, Maslovski S I, Nefedov I S, Silveirinha M G, Simovski C R and Tretyakov S A 2003 Strong spatial dispersion in wire media in the very large wavelength limit *Phys. Rev.* B **67** 113103
[17] Belov P A, Tretyakov S A and Viitanen A J 2002 Dispersion and reflection properties of artificial media formed by regular lattices of ideally conducting wires *J. Electromagn. Waves Appl.* **16** 1153–70
[18] Taflove A 2000 *Computational Electrodynamics: The Finite-Difference Time-Domain Method* 2nd edn (Norwood, MA: Artech House Publishers)
[19] Berenger J R 1994 A perfectly matched layer for the absorption of electromagnetic waves *J. Comput. Phys.* **114** 185–200
[20] Zhao Y, Belov P A and Hao Y 2007 Modelling of wave propagation in wire media using spatially dispersive finite-difference time-domain method: numerical aspects *IEEE Trans. Antennas Propag.* **55** 3070–7
[21] Tyo J S 2003 A class of artificial materials isorefractive with free space *IEEE Trans. Antennas Propag.* **51** 1093
[22] Hu X, Chan C T, Zi J, Li M and Ho K-M 2006 Diamagnetic response of metallic photonic crystals at infrared and visible frequencies *Phys. Rev. Lett.* **99** 223901
[23] Shin J, Shen J-T, Catrysse P B and Fan S 2006 Cut-through metal slit array as an anisotropic metamaterial film *IEEE J. Sel. Top. Quantum Electron.* **12** 1116–22
[24] Silveirinha M G 2006 Nonlocal homogenization model for a periodic array of ε-negative rods *Phys. Rev.* E **73** 046612